Pis'ma v ZhETF, vol. 92, iss. 10, pp. 715 – 719 © 2010 November 25

Consistent α-cluster description of the $^{12}\mathrm{C}(0_2^+)$ "Hoyle" resonance

S. I. Fedotov, O. I. Kartavtsev, A. V. Malykh

Joint Institute for Nuclear Research, 141980 Dubna, Russia

Submitted 30 September 2010

The near-threshold $^{12}\mathrm{C}(0_2^+)$ resonance provides unique possibility for fast helium burning in stars, as predicted by Hoyle to explain the observed abundance of elements in the Universe. Properties of this resonance are calculated within the framework of the α-cluster model whose two-body and three-body effective potentials are tuned to describe the $\alpha-\alpha$ scattering data, the energies of the 0_1^+ and 0_2^+ states, and the 0_1^+-state root-mean-square radius. The extremely small width of the 0_2^+ state, the $0_2^+ \to 0_1^+$ monopole transition matrix element, and transition radius are found in remarkable agreement with the experimental data. The 0_2^+-state structure is described as a system of three α-particles oscillating between the ground-state-like configuration and the elongated chain configuration whose probability exceeds 0.9.

The extremely narrow $^{12}\mathrm{C}(0_2^+)$ resonance just above the 3α threshold was predicted by Hoyle [1] to explain the observed abundance of elements in the Universe. Following the prediction, the near threshold 3α ($^{12}\mathrm{C}(0_2^+)$) and 2α ($^{8}\mathrm{Be}$) resonances are crucial for sufficiently fast carbon production in stellar nucleosynthesis which goes through the reactions

$$3\alpha \to {}^{8}\mathrm{Be} + \alpha \to {}^{12}\mathrm{C}(0_2^+) \to {}^{12}\mathrm{C} + \gamma.$$

The experimental confirmation came soon [2] and properties of this state have been fairly well studied experimentally during the following 50 years. In particular, the extremely small width Γ and the $0_2^+ \to 0_1^+$ transition density (the monopole transition matrix element M_{12} and the transition radius R_{12}) were determined. Besides the resonance triple-α reaction, a consistent treatment of the three-body near-threshold dynamics is ultimately necessary to study the non-resonance reaction, which is of importance at low temperature and high helium density, as occurs in accretion on white dwarfs and neutron stars [3]. As the experimental data at these conditions are lacking, the reliable theoretical results are especially desired; nevertheless, the calculated non-resonance reaction rates [4 – 7] differ by many orders of magnitude. There is vast literature on the $^{12}\mathrm{C}$ states above the 3α threshold, and it is possible to notice just some of the recent papers, e. g., with concern of astrophysical aspects [7 – 9], distribution of decaying particles [10, 11], dilute-gas variational calculations [12], and different approaches to precise description of the $^{12}\mathrm{C}$ properties [13 – 17]. Besides much interest in the $^{12}\mathrm{C}(0_2^+)$ state owing to its role in the astrophysical applications, the structure of this state has been widely discussed for a long time, in particular, a linear chain configuration was suggested in [18] and a triangle configuration was considered in [19].

The following reasons impede the theoretical description of the $^{12}\mathrm{C}(0_2^+)$ resonance and, more generally, of the 3α low-energy processes. Application of the twelve-nucleon calculations is hardly feasible for the unstable near-threshold 0_2^+ state; the extremely difficult task is to describe the α-cluster structure and complicated three-body dynamics of α-particles. On the other hand, although the α-cluster model is a natural alternative and a number of works have elaborated in this direction, it remains to prove that the model would provide the desired accuracy. One of the crucial difficulties stems from the three-body decay of the 0_2^+ resonance, which requires the construction of the asymptotic wave function for three charged particles.

The present Letter is aimed at reliable calculation of the $^{12}\mathrm{C}(0_2^+)$ resonance within the framework of the α-cluster model with particular intention to obtain its extremely small width Γ and the experimentally observable monopole transition matrix element M_{12} and transition radius R_{12}. Moreover, the reliable α-cluster calculation will be used to elucidate the 0_2^+-state structure. The α-cluster model is applied also to calculate the 0_1^+ state despite that its cluster structure is not justified. First, this calculation provides a consistent treatment of the 0_2^+–0_1^+ transition as the wave functions of both states should be calculated within the same approach. Next, it is of importance for a correct description of those effects which originate from the α-particles structure. An additional goal of the $^{12}\mathrm{C}(0_2^+)$ calculation is to construct the effective potentials of the α-cluster model which is known to be successful in different nuclear problems. The focus of the present calculation is the precise solution of the three-body problem which allows one to show an ultimate ability of the α-cluster model in description of the fine $^{12}\mathrm{C}$ characteristics.

For a precise description of the ^{12}C nucleus, firstly, the effective three-body interaction is introduced to take into account the finite size and nucleonic structure of the α-particles including the effects of wave-function antisymmetrization under nucleons. Next, the assumption on the "frozen" nucleon distribution in the α-particles is used to calculate the experimentally observable nucleonic structural characteristics, e. g., the root-mean-square (r. m. s.) radii and the transition radius R_{12}. This extended α-cluster model leads generally to a satisfactory description of the ^{12}C nucleus [10, 13 – 15, 20]. In particular, the calculated Γ and M_{12} [13, 14] are in reasonable agreement with experimental data (up to a factor two) even for the simplified local α–α interactions.

The effective potentials of the α-cluster model are constructed under the following natural requirements. The two-body potential is chosen to reproduce the low-energy elastic-scattering phase shifts in the lowest even-parity waves and to fix at the experimental values both energy and width of the narrow α-α resonance (the ^{8}Be ground state). The latter condition is essential for a correct description of the multi-dimensional potential barrier whose penetrability determines the extremely small width Γ of the ^{12}C(0_2^+) state. Furthermore, for any reasonable calculation of the width Γ, the 0_2^+-state energy should be precisely fixed to the experimental value by a proper choice of the effective three-body potential. As the ground-state wave function is needed to treat the 0_2^+–0_1^+ transition, the effective three-body potentials should provide also the experimental values of the energy and r. m. s. radius of the 0_1^+ state.

The Schrödinger equation reduces to the system of coupled hyperradial equations (HRE) for the channel functions $f_n(\rho)$ by using the expansion of the three-body wave function in a set of eigenfunctions $\Phi_n(\alpha,\theta;\rho)$ on a hypersphere at fixed ρ,

$$\Psi = \rho^{-5/2}\sum_{n=1}^{\infty} f_n(\rho)\Phi_n(\alpha,\theta;\rho). \qquad (1)$$

Here the hyperspherical variables $0 \le \rho < \infty$, $0 \le \alpha_i \le$ $\le \pi$, and $0 \le \theta_i \le \pi$ are defined by $x_i = \rho\cos(\alpha_i/2)$, $y_i = \rho\sin(\alpha_i/2)$, and $\cos\theta_i = (\mathbf{x}_i\cdot\mathbf{y}_i)/(x_i y_i)$, the scaled Jacobi coordinates are $\mathbf{x}_i = \mathbf{r}_j - \mathbf{r}_k$, $\mathbf{y}_i =$ $= (2\mathbf{r}_i - \mathbf{r}_j - \mathbf{r}_k)/\sqrt{3}$ and $\mathbf{r}_i$ is the position of the ith α-particle. Both the total wave function Ψ and the eigenfunctions $\Phi_n(\alpha,\theta;\rho)$ are symmetrical under any permutation of the α-particles. In more detail, the method of calculation and the numerical procedure are presented in [13, 14].

The two-body interaction includes the Coulomb part, $4e^2/x$, and the short-range part of the simple Ali-Bodmer form,

$$V(x) = V_r e^{-x^2/\mu_r^2} + V_a e^{-x^2/\mu_a^2}, \qquad (2)$$

in the s, d, and g partial waves. Following the above discussed requirements, the parameters of the two-body potentials are chosen to fit the low-energy α–α elastic-scattering phase shifts (up to $E_{\mathrm{cm}} = 12$ MeV) and to reproduce the experimental energy $E_{2\alpha} = 92.04 \pm 0.05$ keV and width $\gamma = 5.57 \pm 0.25$ eV of the ^{8}Be ground state [21, 22]. These conditions do not uniquely fix the two-body interactions and to elucidate its role two variants are considered for each of the s-, d-, and g-wave potentials whose parameters are listed in Table 1. Given

Table 1

Parameters $V_{r,a}$ and $\mu_{r,a}$ of the α–α potential (2) for two variants in each of the $l = 0, 2, 4$ partial waves

l		V_r (MeV)	μ_r (fm)	V_a (MeV)	μ_a (fm)
0	s0	234.914	1.54	−109.766	2.0944
0	s1	295.160	1.4213	−99.1406	2.09455
2	d0	152.9	1.4213	−99.1406	2.09455
2	d1	240.0	1.3	−99.1406	2.09455
4	g0	10.0	1.424	−134.0	2.09455
4	g1	36.0	1.424	−140.0	2.09455

the two-body potential, the corresponding three-body potential of the Woods-Saxon form,

$$V_3(\rho) = \frac{V_0}{1 + e^{(\rho-a)/b}}, \qquad (3)$$

is chosen to fix the 0_1^+-state energy, the 0_2^+-state energy, and the 0_1^+-state r. m. s. radius at the experimental values $E_1 = -7.2747$ MeV, $E_2 = 0.3795$ MeV [23], and $R_1 = 2.48 \pm 0.002$ [24, 25]. Five of eight possible combinations of the two-body potentials under consideration, which provide the desired E_1, E_2, and R_1, and fitted parameters V_0, a, and b of the three-body potential (3) are presented in Table 2.

A set of eigenfunctions $\Phi_n(\alpha,\theta;\rho)$ and all the terms in the HRE are obtained by using the variational method with a flexible basis of symmetrical (under any permutation of three particles) trial functions. For small $\rho \le 20$ fm, sufficient precision is achieved on the basis containing 192 (corresponding to $K_{\max} = 90$) symmetrical hyperspherical harmonics (SHH). With increasing ρ, a number of SHH providing the desired accuracy enormously grows due to the $\alpha + {}^8$Be cluster structure of the wave function. Therefore, the desired precision is obtained with the basis containing a set of 108 SHH

Table 2

	V_0	a	b	Γ	R_2	M_{12}	R_{12}
A	−33.7737	2.87500	0.97565	8.29	3.555	5.270	4.844
B	−50.5656	2.23438	1.05366	8.51	3.572	5.278	4.852
C	−129.031	0.96875	1.11313	8.65	3.576	5.449	4.847
D	−63.4126	1.90625	1.06614	7.92	3.574	5.335	4.836
E	−109.009	1.15234	1.1075	8.71	3.590	5.298	4.843

The 0_2^+ state width Γ (eV), the r. m. s. radius R_2 (fm), the monopole transition matrix element M_{12} (fm^2), and the transition radius R_{12} (fm). The combinations of the two-body potential are denoted as (A) for (s0 d0 g0), (B) for (s0 d0 g1), (C) for (s0 d1 g0), (D) for (s1 d0 g0), and (E) for (s1 d0 g1) in accordance with Table 1. Parameters of the corresponding three-body potential (3) are V_0 (MeV), a (fm), and b (fm).

(corresponding to $K_{\max} = 66$) and four additional trial functions $\varphi_j = \sum_i \exp\left(-\beta_j x_i^2\right)$.

Whereas the simple zero asymptotic boundary conditions in the HRE are used in the calculation of the 0_1^+ state, the complicated scattering problem for three charged particles should be solved to describe the 0_2^+ resonance. Fortunately, the $\alpha+{}^8$Be two-cluster structure of the wave function at large, though finite, distances is corroborated in the present calculations, which allows one to circumvent the tremendous calculation of the three-charged-particle wave function. The $\alpha + {}^8$Be structure follows from the form of $\Phi_1(\alpha,\theta;\rho)$ which is close to the symmetrized combination $\sum_i \phi(x_i)$ of the ^{8}Be wave function $\phi(x)$ in a wide region 20 fm $\le \rho \le$ 70 fm, where the overlap integral on a hypersphere $\langle\Phi_1|\sum_i \phi(x_i)\rangle$ exceeds 0.977. This form of $\Phi_1(\alpha,\theta;\rho)$ is demonstrated in Fig.1 for $\rho = 30$ fm, where three peaks represent the

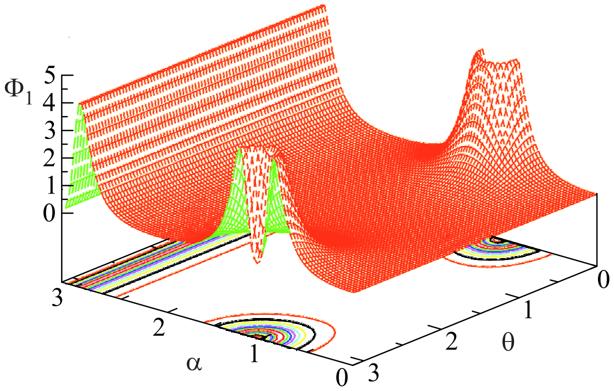

Fig.1. The eigenfunction $\Phi_1(\alpha,\theta;\rho)$ at $\rho = 30$ fm

functions $\phi(x_i)$. The two-cluster structure is approved also by the form of the first-channel effective potential in the HRE, which to good accuracy is a sum of the ^{8}Be energy $E_{2\alpha}$ and the Coulomb interaction between α and ^{8}Be, $2\eta e^2/\rho$ in the interval 40 fm $< \rho <$ 70 fm. Indeed, fit to this dependence gives 89.29 keV $< E_{2\alpha} <$ 90.4 keV and $6.73 < \eta < 6.76$ which are close to the expected values $E_{2\alpha} = 92.04 \pm 0.05$ keV and $\eta = 8/\sqrt{3} \approx 6.65$. Thus, the 0_2^+-state properties are calculated by using the two-cluster ($\alpha + {}^8$Be) asymptotic boundary condition for the first-channel function $f_1(\rho)$ at a large, though finite, hyperradius. More precisely, the asymptotic form is $f_1(\rho) \propto F_0(\eta/kr_b, k\rho) + \tan\delta(E) G_0(\eta/kr_b, k\rho)$, where $\delta(E)$ is the scattering phase shift, F_0 and G_0 are the Coulomb functions, $k^2 = (m_\alpha/\hbar^2)(E - E_{2\alpha})$, and $r_b = \hbar^2/m_\alpha e^2$. The 0_2^+-state energy E_2 and width Γ are obtained by fitting $\delta(E)$ to the Wigner energy dependence.

The assumption on the fixed nucleon distribution in the α-particle leads to the representation of the twelve-nucleon wave function as a product of the three-body wave function Ψ and the internal wave functions of the three α-particles. Using this form, one obtains from the usual definitions [13, 14, 26] that the monopole transition matrix element is expressed merely via the three-body wave functions,

$$M_{12} = \langle \Psi^{(1)} \left|\rho^2\right| \Psi^{(2)} \rangle, \tag{4}$$

whereas the r. m. s. radii and the transition radius depend also on the α-particle r. m. s. radius $R_\alpha = 1.681 \pm 0.004$ fm [27], viz.:

$$R_i^2 = \frac{1}{6}\langle \Psi^{(i)} \left|\rho^2\right| \Psi^{(i)} \rangle + R_\alpha^2 \tag{5}$$

and

$$R_{12}^2 = \frac{\langle \Psi^{(1)} \left|\rho^4 \left(3 - \sin^2\alpha \sin^2\theta\right)\right| \Psi^{(2)} \rangle}{12 M_{12}} + \frac{10}{3} R_\alpha^2. \tag{6}$$

In calculation of M_{12} (4), R_2 (5), and R_{12} (6) the ultra-narrow 0_2^+-resonance is treated as a bound state, whose wave function $\Psi^{(2)}$ is taken as a scattering solution at the resonance energy E_2 normalized on the interval $\rho \le \rho_t$, where $\rho_t \approx 45$ fm is the typical extention of the potential barrier.

The solution of the five-channel system of HREs provides the desired accuracy for Γ, M_{12}, R_{12}, and R_2 which are presented for all the selected potentials in Table 2. Amazingly, both Γ and M_{12} coincide with the measurements 8.5 ± 1.0 eV [23] and 5.48 ± 0.22 fm^2 [26] within the experimental errors, while the calculated R_{12} slightly overestimates the experimental value 4.396 ± 0.27 fm [26]. The recent experiment [28] of significantly improved accuracy gives $M_{12} = 5.47 \pm 0.09$ fm^2 and $R_{12} = 4.59 \pm 0.16$ fm, still the calculated M_{12} is in agreement with these highly accurate data, whereas R_{12} agrees even better. Thus, the quite natural requirements on the simple two-body and three-body effective potentials of the α-cluster model turn out to be sufficient for a precise description of the lowest ^{12}C(0^+) states. The reliable value of the 0_2^+-state r. m. s. radius is found with a small variance about $R_2 = 3.57$ fm which exceeds R_1 more than 1 fm. Note that the exact experimental data on R_2 are not available and the efforts to extract its value, e. g., from the Fraunhofer diffraction in the inelastic $\alpha +^{12}$ C scattering, are affected by the model assumptions [29].

A stark success in the calculation of the Γ, M_{12}, and R_{12} implies that the α-cluster model provides a good description of the 0_2^+ state's structure. The structural properties become more conspicuous, if represented in the variables ξ and φ_i defined by the expressions $\sin\xi = \sin\alpha_i \sin\theta_i$ and $\cos\xi\cos\varphi_i = \cos\alpha_i$. As the inertia momenta

$$I_1 = \frac{1}{2} m_\alpha \rho^2 \cos^2\frac{\xi}{2}, \quad I_2 = \frac{1}{2} m_\alpha \rho^2 \sin^2\frac{\xi}{2} \tag{7}$$

are related to ρ and ξ, the probability distribution of α-particles

$$P(\rho,\xi) = \frac{1}{32}\rho^5 \sin 2\xi \int d\varphi |\Psi(\rho,\xi,\varphi)|^2 \tag{8}$$

is plotted in Fig.2 to represent the features of the 0_2^+ state. The sufficiently wide main peak corresponds to

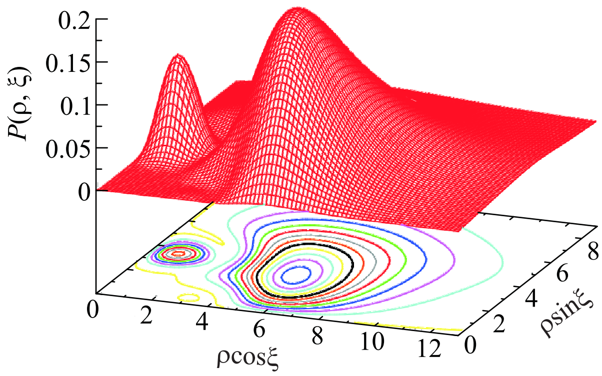

Fig.2. Probability distribution of α-particles $P(\rho,\xi)$ (8) for the ^{12}C(0_2^+) state

different configurations of large size, mostly satisfying the condition $I_2 \gg I_1$, in particular, $P(\rho,\xi)$ takes the maximum for the ratio $I_2/I_1 \approx 18$ and $\rho = 6.3$ fm. In other words, the elongated chain configuration is the most probable shape of the 0_2^+ state. The peak extends to a ridge in the direction of increasing I_2/I_1 which clearly represents the $\alpha + {}^8$Be decay mode. The minor peak is quite similar to the 0_1^+-state probability distribution whose form is consistent with the equilateral triangle configuration. The two peaks are separated by a ravine pointing out at the position of the nodal surface which separates the regions of different sign of the wave-function. This means that three α-particles in the 0_2^+ state oscillate between the ground-state-like configuration and the linear chain configuration which prevails in the total probability, whereas the weight of the minor-peak region is about 7–9%. A detailed and lengthy discusssion of the 0_2^+ state structure is beyond the scope of this Letter and will be given elsewhere.

In summary, it is shown that the α-cluster model, in spite of its relative simplicity, provides a consistent description of the lowest ^{12}C(0^+) states. Even for the simple effective potentials describing the α-α scattering data, the energy and width of ^{8}Be, the energies of ^{12}C$(0_{1,2}^+)$ states, and the 0_1^+ r. m. s. radius, the calculated 0_2^+ state width Γ, the monopole transition matrix element M_{12}, and the transition radius R_{12} are in excellent agreement with the experimental data. The wave function of the 0_2^+ state corresponds to the system of three α-particles which oscillate between the equilateral triangle and the linear chain configurations, the latter contributing to the total probability about 90%. The three-body calculation directly approves the sequential decay mechanism (^{12}C $\to \alpha + {}^8$Be $\to 3\alpha$) of the 0_2^+ state in agreement with the experiment [30].

The present results indicate that the theoretical calculations within the framework of the α-cluster model are accurate enough to keep pace with the experimental data. There is enough room for further refinement of the α-cluster model which could be used to describe both the improved experimental data and those reactions which depend sensitively on the fine details of the wave function. Important examples could be the α–α bremsstrahlung and the (α, α) reactions. Furthermore, the present approach is promising to study the triple-α reaction ($3\alpha \to {}^{12}$C) at low energy below the three-body resonance that provides an opportunity for unified treatment of the crossover from the resonant to the non-resonant mechanism of the reaction.

1. F. Hoyle, Astrophys. J. Suppl. **1**, 121 (1954).
2. C. W. Cook, W. A. Fowler, C. C. Lauritsen, and T. Lauritsen, Phys. Rev. **107**, 508 (1957).
3. A. G. W. Cameron, Astrophys. J. **130**, 916 (1959).
4. K. Nomoto, F.-K. Thielemann, and S. Miyaji, Astron. Astrophys. **149**, 239 (1985).
5. I. Fushiki and D. Q. Lamb, Astrophys. J. **317**, 368 (1987).
6. S. Schramm, K. Langanke, and S. E. Koonin, Astrophys. J. **397**, 579 (1992).

7. K. Ogata, M. Kan, and M. Kamimura, Prog. Theor. Phys. **122**, 1055 (2009).
8. H. Oberhummer, A. Csótó, and H. Schlattl, Science **289**, 88 (2000).
9. H. O. U. Fynbo, C. A. Diget, U. C. Bergmann et al., Nature **433**, 136 (2005).
10. R. Álvarez-Rodríguez, A. S. Jensen, E. Garrido et al., Phys. Rev. C **77**, 064305 (2008).
11. O. S. Kirsebom, M. Alcorta, M. J. G. Borge et al., Phys. Rev. C **81**, 064313 (2010).
12. Y. Funaki, A. Tohsaki, H. Horiuchi et al., Eur. Phys. J. A **28**, 259 (2006).
13. S. I. Fedotov, O. I. Kartavtsev, V. I. Kochkin, and A. V. Malykh, Phys. Rev. C **70**, 014006 (2004).
14. S. I. Fedotov, O. I. Kartavtsev, and A. V. Malykh, Eur. Phys. J. A **26**, 201 (2005).
15. I. Filikhin, V. M. Suslov, and B. Vlahovic, J. Phys. G **31**, 1207 (2005).
16. M. Chernykh, H. Feldmeier, T. Neff et al., Phys. Rev. Lett. **98**, 032501 (2007).
17. P. Descouvemont, J. Phys. G **37**, 064010 (2010).
18. D. M. Brink, H. Friedrich, A. Weiguny, and C. W. Wong, Phys. Lett. B **33**, 143 (1970).
19. R. Bijker and F. Iachello, Phys. Rev. C **61**, 067305 (2000).
20. R. Álvarez-Rodríguez, E. Garrido, A. S. Jensen et al., Eur. Phys. J. A **31**, 303 (2007).
21. S. Wüstenbecker, H. W. Becker, H. Ebbing et al., Z. Phys. A **344**, 205 (1992).
22. D. R. Tilley, J. H Kelley, J. L. Godwin et al., Nucl. Phys. A **745**, 155 (2004).
23. F. Ajzenberg-Selove, Nucl. Phys. A **506**, 1 (1990).
24. E. A. J. M. Offermann, L. S. Cardman, C. W. de Jager et al., Phys. Rev. C **44**, 1096 (1991).
25. W. Ruckstuhl, B. Aas, W. Beer et al., Nucl. Phys. A **430**, 685 (1984).
26. P. Strehl and T. H. Schucan, Phys. Lett. B **27**, 641 (1968).
27. I. Sick, Phys. Rev. C **77**, 041302 (2008).
28. M. Chernykh, H. Feldmeier, T. Neff et al., Phys. Rev. Lett. **105**, 022501 (2010).
29. A. N. Danilov, T. L. Belyaeva, A. S. Demyanova et al., Phys. Rev. C **80**, 054603 (2009).
30. M. Freer, A. H. Wuosmaa, R. R. Betts et al., Phys. Rev. C **49**, R1751 (1994).